

Design and analysis of biomimetic joints for morphing of micro air vehicles

This content has been downloaded from IOPscience. Please scroll down to see the full text.

2010 Bioinspir. Biomim. 5 045007

(<http://iopscience.iop.org/1748-3190/5/4/045007>)

View [the table of contents for this issue](#), or go to the [journal homepage](#) for more

Download details:

IP Address: 128.227.6.132

This content was downloaded on 13/02/2014 at 18:47

Please note that [terms and conditions apply](#).

Design and analysis of biomimetic joints for morphing of micro air vehicles

Daniel T Grant, Mujahid Abdulrahim and Rick Lind

Department of Mechanical and Aerospace Engineering, University of Florida,
Gainesville, FL 32611, USA

E-mail: ricklind@ufl.edu

Received 5 March 2010

Accepted for publication 27 August 2010

Published 24 November 2010

Online at stacks.iop.org/BB/5/045007

Abstract

Flight capability for micro air vehicles is rapidly maturing throughout the aviation community; however, mission capability has not yet matured at the same pace. Maintaining trim during a descent or in the presence of crosswinds remains challenging for fixed-wing aircraft but yet is routinely performed by birds. This paper presents an overview of designs that incorporate morphing to enhance their flight characteristics. In particular, a series of joints and structures is adopted from seagulls to alter either the dihedral or sweep of the wings and thus alter the flight characteristics. The resulting vehicles are able to trim with significantly increased angles of attack and sideslip compared to traditional fixed-wing vehicles.

(Some figures in this article are in colour only in the electronic version)

1. Introduction

The concept of a micro air vehicle (MAV) has rapidly transitioned from a speculative idea to a common platform. Indeed, such vehicles are routinely being designed and flown at numerous universities and government laboratories while industry has already marketed several platforms for military and civilian purposes. Associated flight testing has amply demonstrated their basic capabilities and flight properties [6, 12, 14, 24–28].

Mission capability, unfortunately, lags relatively far beyond flight capability for any current type of MAV. The small size and high agility of these vehicles are highly desired as enabling technologies for flight within dense obstacles of urban environments; however, the ability to precisely follow a trajectory that requires agile maneuvering is a critical need that remains challenging. Many flight operations are thus limited to somewhat benign maneuvers that avoid excessive aerobatics.

This paper introduces a set of vehicles that incorporate avian characteristics to enhance mission capability. Specifically, the designs use joints and structures to greatly enhance agility and improve metrics related to mission effectiveness. Each vehicle uses an elbow and wrist to admit varied wing configurations along with twist to alter the shape of the wing. The rotations of these joints are vertical, such

that the wing tip rotates above the fuselage in the direction of a roll, for one aircraft and horizontal, such that the wing tip rotates forward toward the nose in the direction of a yaw, for the other. In each case, both symmetric and asymmetric morphing can be achieved.

Birds are remarkably appropriate as an inspiration for MAVs. Certainly many birds, such as the laughing gull, have similar size and airspeed to these aircraft. The incorporation of bio-mimetic joints stems from observations of gliding flight. Rapid accelerations and flight path variations are achieved through articulation of the skeletal structure to promote favorable aerodynamic properties. This skeletal structure can be simplified to a system of linkages and joints to achieve a similar effect in aircraft. As such, biologically-inspired morphing is directly achievable.

2. Biological inspiration

2.1. Observations

Gliding birds are able to achieve a wide range of maneuvers and flight paths due, at least in part, to aerodynamic effects related to their geometric configuration of wing and tail. As such, observations of gliding flight provide insight about the motivation for wing shapes incurred during flight. The bird species of particular interest is the laughing gull, *Larus*



Figure 1. Various wing configurations of laughing gulls (*Larus atricilla*) during gliding flight with elbow rotation near the root location and wrist rotation near the mid-span location.

atricilla, because of the close similarities in size and shape to a class of aircraft that is easily constructed. Also, these gulls spend a considerable duration of each flight in various gliding maneuvers so they do sometimes utilize a fixed-wing configuration as opposed to constantly flapping.

These birds use several types of wing morphing to control flight parameters such as glide speed [34], longitudinal pitch stability [17] and lateral yaw stiffness [22]. It is established that planform shape relates to gliding speed for similar glide angles [34]. Yaw stiffness is shown to increase with aft sweep and is sufficiently high such that birds do not require vertical stabilizers [22]. Also, aft rotation of the outboard wing is such that the aerodynamic center typically moves aft which increases the pitch stiffness for operation at higher airspeed [17]. Such morphing to increase aerodynamic efficiency is biologically advantageous because it directly reduces the muscular energy required to maneuver and thus increases metabolic efficiency for the bird [30].

Many configurations used by birds are symmetric about the body such that each wing generates similar aerodynamics; however, asymmetric configurations are definitely used in certain instances of gliding flight. Such asymmetries are advantageous in generating moments for maneuvering, rejecting disturbances and allowing efficient trim at large angles of sideslip [21, 22, 29, 34, 35].

The achievable range of configurations for an avian wing is quite large, although only a subset of the shapes is used in flight. Figure 1 shows several examples of seagull wing configurations during gliding flight. The top row shows two configurations where the joints are mostly articulated vertically about longitudinal joint axes. Dihedral and anhedral angles are varied along each part of the wing to produce the classical ‘gull-wing’ shape. The bottom row shows three configurations with different horizontal joint articulations. In each case, the wing area and shape are dramatically altered due primarily to rotation about joints.

2.2. Avian morphology studies

Recent research on the aerodynamic and dynamic characteristics of birds has quantified the motivation behind

some of the wing shape changes observed in nature. Tucker reported in 1970 on the effect of wing planform shape on the glide angle and glide speed of falcons [32, 33]. Forward sweep of the shoulder or elbow joints and aft sweep of the wrist joint, as in figure 1, are used in varying degrees to control the planform area and wingspan. Such variations of forward sweep and aft sweep serve to alter the dihedral effect without moving the aerodynamic system and, consequently, admit relative differences in effect on damping and associated stability for the longitudinal dynamics and lateral-directional dynamics. Also, the subsequent trim airspeed varies substantially to afford control over loitering or attack speeds.

Sachs reported findings on the role of aft wingtip sweep in providing yaw stiffness and yaw stability on the aerodynamic and inertial scales of bird flight [21]. The aft wing sweep also affects the location of the aerodynamic center and contributes to pitch stability [29]. The results partly explain the stability motivations for swept shapes adopted by birds during high-speed dives.

Joint angle articulation along longitudinal axes has been shown by Davidson to increase the lift to drag ratio substantially on a seagull-inspired wing model [9]. Alternate joint configurations have been shown to have the opposite effect and reduce lift to drag, allowing steep dives at moderate airspeeds [1].

The wing geometry of several bird species is presented by Liu *et al* in 2006 [16]. Three-dimensional scanners are used to generate models of bird wings throughout the flapping cycle. The wing geometries are presented as time-dependent Fourier series, which represent the change in the aerodynamic shape resulting from skeletal articulation. The authors use a two-jointed arm model as a simplification of bird bone structure. The arm model is characterized by three angles and achieves a sufficient range of motion to represent the flapping cycle. The wing surface is assumed to be fixed to one of two spars at the quarter-chord position and maintains proper orientation relative to the flow for all configurations. Although the research focused on flapping flight, the identified wing shapes may also be useful for gliding operations.

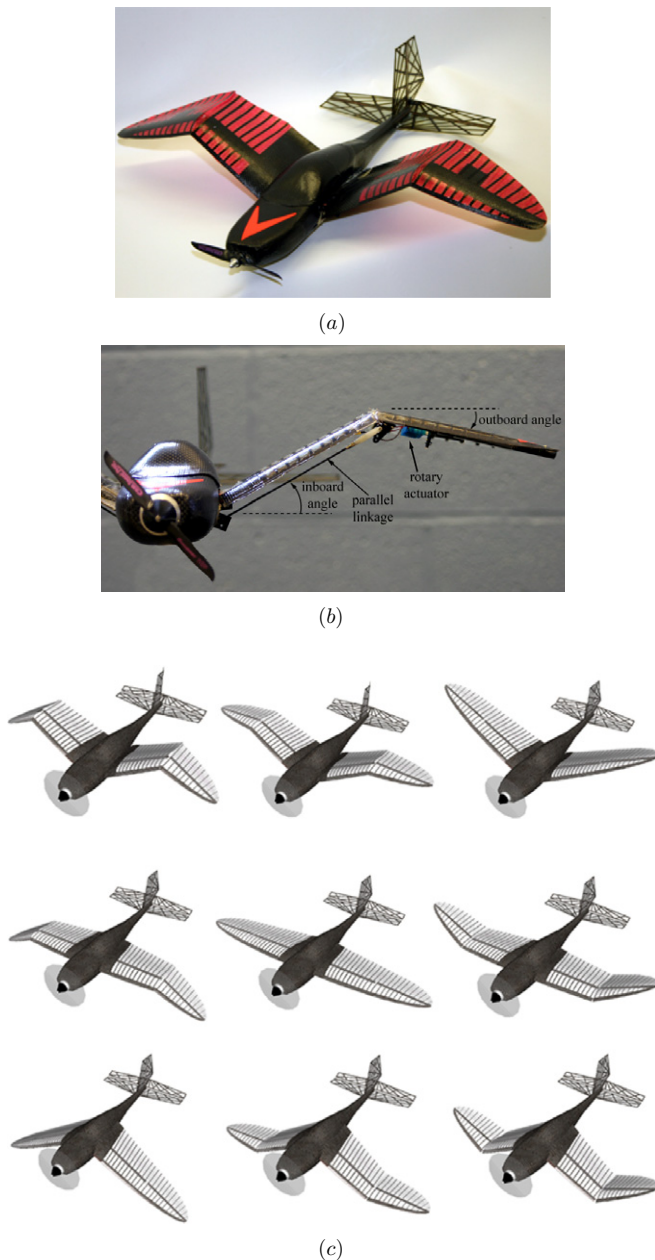


Figure 2. Variable gull-wing aircraft. (a) Overview of vehicle. (b) Left wing with an inboard angle of $\mu_1 = 30^\circ$ and an outboard angle of $\mu_2 = -12^\circ$. (c) Range of configurations.

3. Aircraft

3.1. Multi-joint variable gull-wing aircraft

A vehicle, shown in figure 2(a), is designed to utilize variable gull-wing morphing. This form of morphing allows the inboard and outboard wing sections to be rotated along an axis parallel with the longitudinal direction. The motion is symmetric about the fuselage centerline and allows the inboard and outboard angles to be manipulated independently. The vehicle is able to achieve a variety of configurations ranging from conventional dihedral to a gull wing that resembles the shape of bird wings in gliding flight.

Gull-wing morphing results from angular variations in a 4-joint spar system where all joint axes extend longitudinally. An inboard spar on each wing connects the elbow-type joint at the wing root to the wrist-type joint at a mid-span location. An outboard spar on each wing then connects the wrist-type joint to the wing tip. Each joint has the freedom to rotate in a positive direction or negative direction. An example of such a deflection is shown in figure 2(b) which has a positive angle, $\mu_1 = 30^\circ$, for the elbow joint and a negative angle, $\mu_2 = -12^\circ$, for the wrist joint.

The aircraft is allowed to vary its gull-wing morphing over a range of $-30^\circ \leq \mu_1 \leq 30^\circ$ and $-30^\circ \leq \mu_2 \leq 30^\circ$. Several elements of this configuration space are shown in figure 2(c) for computational models. In this figure, μ_1 is constant for each row while μ_2 is constant for each column.

The nominal wingspan of the vehicle is 62 cm and the weight is roughly 450 g. The vehicle is small enough to be generally considered a MAV but is large enough to carry a useful instrumentation payload. The flight vehicle uses a dynamic wing-twist morphing in place of ailerons to effect roll moment [8]. The twisting adds considerable roll control power while maintaining the beneficial effects of the flexible, membrane wing [3]. The aircraft continues to undergo a program of flight testing to demonstrate the variations in flight dynamics that result from using biomimetic joints [1, 2].

3.2. Multi-joint variable wing-sweep aircraft

A vehicle is designed to admit variations in the sweep angle of each wing. The basic construction uses skeletal members of a prepregged, bi-directional carbon fiber weave along with rip-stop nylon. The fuselage and wings are entirely constructed of the weave while the tail features carbon spars covered with nylon. The resulting vehicle has a weight of 596 g and a fuselage length of 48 cm.

The wings actually consist of separate sections which are connected to the fuselage and each other through a system of spars and joints. These joints, as shown in figure 3(a), are representative of an elbow and a wrist which serve to vary the sweep of inboard and outboard. The range of horizontal motion admitted by these joints is approximately $\pm 30^\circ$.

It is noted that conventional aileron control surfaces are omitted from the aircraft's final design. This feature is a direct result of span-wise inconsistencies created by the dynamic range of morphing configurations. Therefore, the wrist joints are designed in such a manner that they allow both horizontal sweep and rolling twist. This motion is accomplished by creating a floating joint that closely mimics the various ranges of motion attainable by an automobile's universal joint.

The wing surface must be kept continuous for any configuration of sweeping because of aerodynamic concerns. This vehicle ensures such continuity by layering feather-like structures, as shown in figure 3(b), within the joint. These structures retract onto each other under the wing when both the inboard and outboard are swept back. Conversely, they create a fan-like cover across the ensuing gap when the inboard is swept back and the outboard is swept forward. The contraction and expansion of the surface area created by these



Figure 3. Multi-joint sweep aircraft. (a) Underside of wing showing joints and spars. (b) Overlapping elements of wing. (c) Range of configurations.

structures is smoothly maintained by a tract and runner system implemented on the outer regions of each member.

Spars, formed from hollow shafts of carbon fiber, are placed along the leading edge of each wing. These spars act

as both a rigid source to maintain the leading-edge curvature and a connection of each independent wing joint. The inboard spar is translated horizontally by a servo-driven linear actuator located inside the fuselage. The inboard spar is then connected

to the inboard wing section at the elbow joint located on the outside of the fuselage. The inboard spar then connects at the wrist joint to outboard spar at roughly the quarter-span point. The outboard wing region is activated independently of the inboard region by means of a servo attached at the wrist.

Overall, this vehicle is able to achieve a wide range of sweep orientations. Some representative configurations are shown in figure 3(c) to demonstrate the range.

4. Modeling methodology

The flight dynamics are analyzed using Athena Vortex Lattice, AVL, to estimate the aerodynamics [10]. This low-order code makes assumptions that the flow is incompressible and inviscid. The community has demonstrated that such assumptions are particularly appropriate for MAVs such as the ones considered in this paper with thin wings [5, 7, 13, 15, 20, 23–26, 31]. The aerodynamics of the wings are estimated along with flow associated with slender bodies such as the fuselage.

AVL assumes quasi-steady flow so unsteady vorticity shedding is neglected. More precisely, it assumes the limit of small reduced frequency which means that any oscillatory motion must be slow enough so that the period of oscillation is much longer than the time it takes the flow to traverse an airfoil chord. This assumption is valid for virtually any expected flight maneuver of the vehicle. Also, the rates in roll, pitch and yaw used in the computations must be slow enough so that the resulting relative flow angles are small. The relative size of these flow angles can be judged by the dimensionless rotation rate parameters, which should fall within the practical limits shown in equation (1):

$$\begin{aligned} -0.10 < pb/2V < 0.10 \\ -0.03 < qc/2V < 0.03 \\ -0.25 < rb/2V < 0.25. \end{aligned} \quad (1)$$

Equation (1) describes the limits at which aircraft motion becomes extremely violent. These limits are unlikely to be exceeded in any typical flight situation, except possibly during low-air-speed aerobatic maneuvers.

5. Mission adaptation for variable gull-wing aircraft

5.1. Steep descent

Flight maneuvers performed in the vicinity of obstacles can require aerodynamic characteristics very different from flight in open environments. Steep descent maneuvers favor relatively inefficient configurations to stabilize the aircraft in a steep descent angle or high rate of descent. The lowest-lift-to-drag and the maximum-power-required configurations achieve the steepest descent and fastest rate of descent maneuvers, respectively.

The steepest angle of descent flight mode is required when large changes in elevation are commanded in areas with limited horizontal space. A descent from building-top level to street level presents such a scenario, where the vehicle must lose considerable altitude within the hard limits of the horizontal

distance between buildings. A steep spiraling flight path can be used to descend quickly without requiring a large flying area.

Figure 4(a) shows one possible configuration for a steep descent mode. The vehicle uses a gull-wing shape with large dihedral on the inboard and large anhedral on the outboard. Wing sweep decreases outward, with the maximum aft sweep on the inboard section and moderate aft sweep on the outboard section. Such a configuration is similar to observed seagull wing shapes used to regulate the glide ratio, where increasing dihedral/anhedral angles decreases the glide ratio [19]. Handling qualities criteria, such as modal damping and frequency that ensure oscillatory motions do not interfere with the mission [11], are used in the selection of the wing shape.

The configuration that achieves the steepest descent angle and maximum rate of descent using the stable dynamics criteria is shown in figure 4(b). The wing uses the maximum dihedral angle for both inboard and outboard wings along with maximum aft sweep for the inboard and moderate aft sweep for the outboard wing. The wing shape is similar to the form used by homing pigeons during the steep descent phase preceding landing. The configuration generated using the unstable dynamics criteria is similar to the stable shape, except that the outboard wing uses the maximum aft sweep.

5.2. Sensor pointing

A UAV engaged in reconnaissance of a moving object or general area may find difficulty in maintaining the target in the sensor field of view. Vision sensors are typically fixed to the aircraft body, which must fly through the air in a particular attitude to maintain an appropriate angle of attack and sideslip. A surveillance mission targeting the face of a building would require that the aircraft fly parallel to the building side where only one part of the sensor field of view is providing useful information. Flying the aircraft toward the building can offer a better perspective, but only allows surveillance for brief periods between circling maneuvers to fly away from and re-acquire the target area in the image.

An alternative approach to the mission is to provide sensor pointing capability by partially decoupling between attitude and velocity. The vehicle would then operate at large sideslip angles in order to fly parallel to the building side while directing the sensor footprint toward the area of interest. The technique would also allow the aircraft to track a moving road vehicle while flying to the side of the roadway.

Trimmed flight at large sideslip requires relatively weak stability derivatives and strong control derivatives. Stiffness and coupled derivatives should be low such that the vehicle is not subject to large yawing and rolling moments. As such, a cost function is formed by these derivatives such that minimizing the cost increases the performance of the vehicle. The minimization is also subject to additional constraints, such as stability, which must be maintained.

Figure 4(c) shows the configuration that is able to fly with the largest angle of sideslip while maintaining stability and controllability. The shape is non-conventional by both

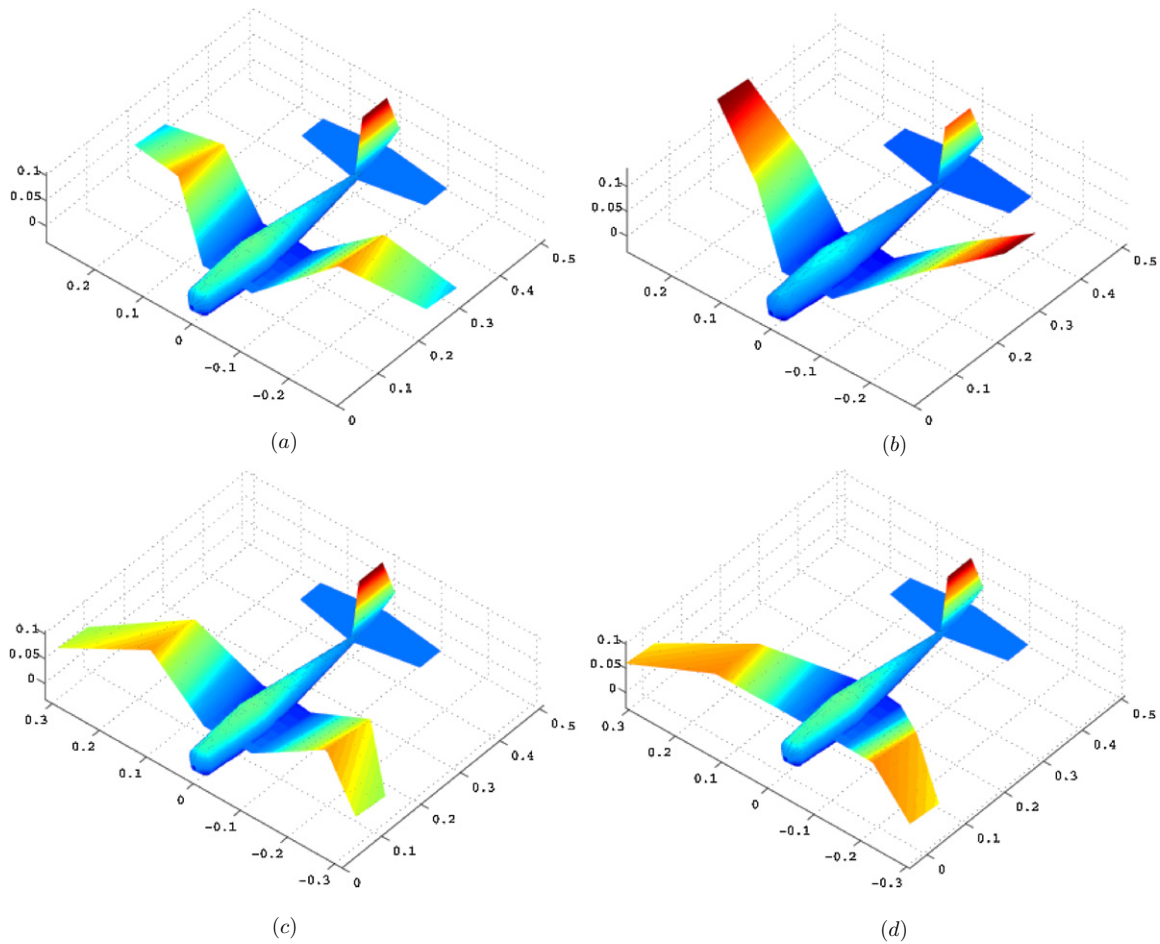


Figure 4. Symmetric configurations for mission performance. (a) Configuration to optimize handling qualities using $\mu_1 = 30^\circ$, $\mu_2 = -30^\circ$, $\mu_3 = -15^\circ$, $\mu_4 = -30^\circ$. (b) Configuration to optimize descent angle using $\mu_1 = 30^\circ$, $\mu_2 = -30^\circ$, $\mu_3 = 30^\circ$, $\mu_4 = -20^\circ$. (c) Configuration to optimize handling qualities using $\mu_1 = 25^\circ$, $\mu_2 = -10^\circ$, $\mu_3 = -10^\circ$, $\mu_4 = 30^\circ$. (d) Configuration to optimize angle of sideslip with relaxed stability using $\mu_1 = 30^\circ$, $\mu_2 = 25^\circ$, $\mu_3 = 0^\circ$, $\mu_4 = 30^\circ$.

biological and aviation standards in that the inboard wings are swept aft while the outboard wings are swept forward. The wing also uses a gull-wing configuration with large dihedral on the inboard and moderate anhedral on the outboard. The unusual orientation of the outboard wings is expected to contribute to the large sideslip constraint. Anhedral wing tips reduce the vehicle tendency to produce a roll moment in response to sideslip [18] while the forward sweep reduces the directional stiffness [4, 21]. The opposite attitude of the inboard wings is used to maintain an appropriate position of the aerodynamic center relative to the vehicle body for the desired dynamic response.

Relaxing the stability criteria to allow unstable dynamics produces a qualitatively similar shape except that the wing tips are not angled downward and are swept forward. Figure 4(d) shows the resulting wing configuration. This unstable configuration produces a moderately divergent spiral mode and a highly divergent short period mode with a time to double of $T_2 = 0.5$ s. The configuration determined by the stable dynamics criteria is similar to the unstable shape with joint angles of $\mu_1 = 30^\circ$, $\mu_2 = 15^\circ$, $\mu_3 = -5^\circ$ and $\mu_4 = 30^\circ$.

Table 1. Configuration ranges for asymmetric sweep.

Wing section	Right wing	Left wing
Inboard (degrees)	0	-30 to 30
Outboard (degrees)	0	-30 to 30

6. Mission adaptation for variable wing-sweep aircraft

6.1. Turn performance

The aircraft’s asymmetric morphing capability can be utilized for enhancing turn characteristics. A mission profile is envisioned requiring that the aircraft be trimmed at a 30° , positive bank angle while being held at constant throttle throughout the turn. As a result, the effective change in forward velocity, and therefore turn radius, due strictly to morphing can be observed. In order to demonstrate the process while facilitating visualization, the design space was limited to the following configurations, as shown in table 1, in which the right wing is fixed with no sweep while the left wing can sweep either forward or rear.

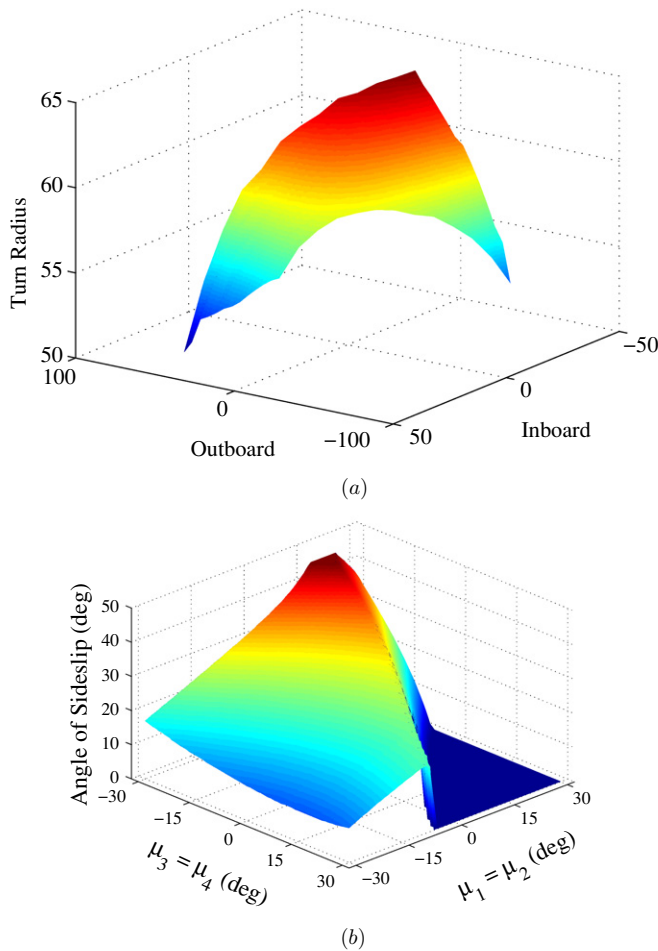


Figure 5. Performance of variable wing-sweep aircraft. (a) Turning radius (m). (b) Maximum angle of sideslip at which aircraft can trim.

The turn radius at which the vehicle can trim is shown in figure 5(a) for each morphing configuration. These results indicate that the turn radius can be decreased by sweeping the wing fully aft. Actually, the greatest reduction in turn radius is achieved by sweeping the inboard section while only minor effect is noted by sweeping the outboard section.

Such a relationship between turn radius and wing sweep is justified by the associated aerodynamics. Essentially, the reduced area of a backward-swept wing induces less drag and thus higher velocities while the converse is true for forward-swept wing. The vehicle is constrained to a constant thrust so the backward-swept configurations must slow down to maintain trim and, consequently, require a smaller radius to turn.

6.2. Crosswind rejection

Sensor pointing in urban environments is a prime mission for which MAVs are being developed. Crosswinds, both steady-state wind and time-varying gusts, present a significant challenge to maintaining sensor pointing during flight. The common approach to sensor pointing despite crosswinds is turning into the wind and crabbing downrange to periodically point the sensor; however, such an approach is certainly not

optimal due to the lack of continuous coverage by the sensor along the desired line of sight.

Asymmetric wing sweep can enhance the ability to perform sensor pointing in the presence of such crosswinds. In particular, one wing can be swept downwind while one wing is swept upwind. The aircraft has, in a sense, rotated the wings into the wind while the fuselage remains pointed in its original direction.

The angle of sideslip at which the aircraft can trim is an indicator of the amount of crosswind in which the aircraft can maintain sensor pointing. A representative demonstration, shown in figure 5(b), presents the maximum positive values for the angle of sideslip at which the aircraft can trim. The wings are constrained in this demonstration such that inboard and outboard angles are identical which limits the degrees of freedom and facilitates presentation. Also, each condition corresponds to the largest angle of sideslip at which the aircraft can trim given deflection limits of $\pm 15^\circ$ for the rudder and elevator along with aileron.

The data in figure 5(b) demonstrate that wing sweep is beneficial for sensor pointing. Specifically, a forward -30° sweep of the left wing and a backward 30° sweep of the right wing allows an angle of sideslip of 44° to be maintained. This maximum angle decreases as the left wing decreases its forward sweep and the right wing decreases its backward sweep. The vehicle is eventually unable to trim at any positive angle of sideslip when both the wings are swept backward.

7. Conclusion

Morphing represents a biologically-inspired approach to aircraft design that has the potential to dramatically enhance mission capability. In particular, MAVs are excellent platforms for morphing given their direct similarities in size and airspeed to birds and bats. The inclusion of biomimetic joints and structures has been shown to enhance a MAV's ability to accomplish certain tasks during common missions. These tasks represent agility and maneuverability exercises such as steep descents, turn performances and crosswind rejection. Computational analysis of a pair of vehicles that use elbow and wrist joints indicates the resulting benefit of this morphing implementation.

Future work on this topic would include in-depth flight tests for each vehicle as well as the eventual development of a six-degree-of-freedom planform utilizing both sweep and dihedral.

References

- [1] Abdulrahim M 2005 Flight performance characteristics of a biologically-inspired morphing aircraft *Proc. AIAA Aerospace Sciences Meeting (Reno, NV, January 2005)* AIAA-2005-345
- [2] Abdulrahim M and Lind R 2004 Flight testing and response characteristics of a variable gull-wing morphing aircraft *Proc. AIAA Guidance Navigation and Control Conf. (Providence, RI, August 2004)* AIAA-2004-5113
- [3] Abdulrahim M, Garcia H and Lind R 2005 Flight characteristics of shaping the membrane wing of a micro air vehicle *J. Aircr.* **42** 131–7

- [4] Barnard R H and Philpott D R 2004 *Aircraft Flight* 3rd edn (Upper Saddle River: NJ, Pearson Education)
- [5] Boschetti P, Cardena E, Amerio A and Arevalo A 2010 Stability and performance of a light unmanned airplane in ground effect *AIAA Aerospace Sciences Meeting* AIAA-2010-293
- [6] De Clercq K, De Kat R, Remes B, van Oudheusden B and Bijl H 2009 Flow visualization and force measurements on a hovering flapping-wing MAV DelFly II *Proc. AIAA Fluid Dynamics Conf.* AIAA-2009-4035
- [7] Cox C, Gopalarathnam A and Hall C E 2009 Development of stable automated cruise flap for an aircraft with adaptive wing *J. Aircr.* **46** 301–11
- [8] Grant D T, Abdulrahim M and Lind R 2006 Flight dynamics of a morphing aircraft utilizing independent multiple-joint wing sweep *AIAA Atmospheric Flight Mechanics Conf. (Keystone, CO, August 2006)* AIAA-2006-6505
- [9] Davidson J B, Chwalowski P and Lazos B S 2003 Flight dynamic simulation assessment of a morphable hyper-elliptic cambered span winged configuration *Proc. AIAA Atmospheric Flight Mechanics Conf. (Austin, TX, August 2003)* AIAA-2003-5301
- [10] Drela M and Youngren H AVL—aerodynamic analysis, trim calculation, dynamic stability analysis, aircraft configuration development (Athena Vortex Lattice) v. 3.15 <http://raphael.mit.edu/avl/>
- [11] Hodgkinson J 1998 *Aircraft Handling Qualities* (Reston, VA: American Institute of Aeronautics and Astronautics)
- [12] Hwang H, Chung D, Yoon K, Park H, Lee Y and Kang T 2002 Design and flight test of a fixed-wing MAV *Proc. AIAA UAV Conf.* AIAA-2002-3413
- [13] Gopalarathnam A and Norris R K 2009 Ideal lift distributions and flap angles for adaptive wings *J. Aircr.* **46** 562–71
- [14] Keennon M and Grasmeyer J 2003 Development of two MAVs and vision of the future of MAV design *Proc. AIAA Int. Air and Space Symp. and Exposition* AIAA-2003-2901
- [15] Leong H I, Jager R, Keshmiri S and Colgren R 2010 Development of a pilot training platform for UAVs using a 6DOF nonlinear model with flight test validation *AIAA Modeling and Simulation Conf.* AIAA-2008-6368
- [16] Liu T, Kuykendoll K, Rhew R and Jones S 2004 Avian wings *Proc. AIAA Aerodynamic Measurement Technology and Ground Testing Conf. (Portland, OR, 28 June–1 July 2004)* AIAA-2004-2186
- [17] Neal D A, Good M G, Johnston C O, Robertshaw H H, Mason W H and Inman D J 2004 Design and wind-tunnel analysis of a fully adaptive aircraft configuration *Proc. AIAA Structures, Structural Dynamics and Materials Conf.* AIAA-2004-1727
- [18] Nelson R C 1998 *Flight Stability and Automatic Control* (Boston, MA: McGraw-Hill)
- [19] Perrin J and Cluzaud J 2001 Winged Migration DVD—ASIN B00000CGNEH, Sony Pictures
- [20] Royer D A, Keshmiri S, Sweeten B C and Jones V 2010 Modeling and sensitivity analysis of the meridian unmanned aircraft *AIAA Infotech@Aerospace* AIAA-2010-3468
- [21] Sachs G 2005 Yaw stability in gliding birds *J. Ornithol.* **146** 191–9
- [22] Sachs G 2005 Why birds and mini-aircraft need no vertical tail *Proc. AIAA Atmospheric Flight Mechanics Conf.* AIAA-2005-5807
- [23] Stanford B, Abdulrahim M, Lind R and Ifju P 2007 Investigation of membrane actuation for roll control of a micro air vehicle *J. Aircr.* **44** 741–9
- [24] Stewart K, Abate G and Evers J 2006 Flight mechanics and control issues for micro air vehicles *AIAA Atmospheric Flight Mechanics Conf.* AIAA-2006-6638
- [25] Stewart K, Wagener J, Abate G and Salichon M 2007 Design of the Air Force Research Laboratory Micro Aerial Vehicle Research Configuration *AIAA Aerospace Sciences Meeting* AIAA-2007-667
- [26] Stewart K, Blackburn K, Wagener J, Czabaranek J and Abate G 2008 Development and initial flight tests of a single-jointed articulated-wing micro air vehicle *AIAA Atmospheric Flight Mechanics Conf.* AIAA-2008-6708
- [27] Stiltner B, Faber J, Llien C, Merrit R and Tanious S 2010 Detailed design, construction and flight tests of a remotely piloted ducted fan MAV *Proc. AIAA Aerospace Sciences Meeting* AIAA-2010-1021
- [28] Thipyopas C and Moschetta J M 2008 From development of micro air vehicle testing research to the prototype of TYTO: low speed biplane MAV *Proc. AIAA Applied Aerodynamics Conf.* AIAA-2008-6250
- [29] Thomas A L R and Taylor G K 2001 Animal flight dynamics: I. Stability in gliding flight *J. Theor. Biol.* **212** 399–424
- [30] Tobalske B W 2001 Morphology, velocity and intermittent flight in birds *Integr. Comp. Biol.* **41** 177–87
- [31] Traub L W 2009 Experimental investigation of annular wing aerodynamics *J. Aircr.* **46** 988–96
- [32] Tucker V A and Parrott G C 1970 Aerodynamics of gliding flight in a falcon and other birds *J. Exp. Biol.* **52** 345–67
- [33] Tucker V A 1987 Gliding birds: the effect of variable wing span *J. Exp. Biol.* **133** 33–58
- [34] Tucker V A and Parrott G C 1970 Aerodynamics of gliding flight in a falcon and other birds *J. Exp. Biol.* **52** 345–67
- [35] Videler J J 2005 *Avian Flight* (Oxford: Oxford University Press)